

Flame fronts in Supernovae Ia and their pulsational stability

S.I. Glazyrin*

Institute for Theoretical and Experimental Physics, Moscow 117218, Russia

S.I. Blinnikov†

*Institute for Theoretical and Experimental Physics, Moscow 117218, Russia
Novosibirsk State University, Novosibirsk 630090, Russia and
VNIIA, Moscow 127055, Russia*

A.D. Dolgov‡

*Institute for Theoretical and Experimental Physics, Moscow 117218, Russia
Novosibirsk State University, Novosibirsk 630090, Russia and
University of Ferrara and INFN, Ferrara 44100, Italy*

The structure of the deflagration burning front in type Ia supernovae is considered. The parameters of the flame are obtained: its normal velocity and thickness. The results are in good agreement with the previous works of different authors. The problem of pulsation instability of the flame, subject to plane perturbations, is studied. First, with the artificial system with switched-off hydrodynamics the possibility of secondary reactions to stabilize the front is shown. Second, with account of hydrodynamics, realistic EOS and thermal conduction we can obtain pulsations when Zeldovich number was artificially increased. The critical Zeldovich numbers are presented. These results show the stability of the flame in type Ia supernovae against pulsations because its effective Zeldovich number is small.

I. INTRODUCTION

Supernovae explosions are among the most spectacular events in the Universe: their energy release significantly mixes the interstellar medium and acts like a driving force in gas dynamics of galaxies and production of cosmic rays. The luminosity of an exploding star becomes comparable with the luminosity of the progenitor galaxy, and allows to observe processes in the most distant regions of the Universe. If regular features of the supernova explosions are found for any subtype of supernovae, it could open a new way to measure cosmological distances and the values of the cosmological parameters.

Despite a long history of investigations of these events the complete understanding of underlying physics is still missing. There are several kind of supernova explosions of different types of the progenitor stars with absolutely different physical phenomena behind them. Here we will consider only one subtype of explosions, namely the thermonuclear explosions. These kind of supernovae is called the supernovae of type Ia, SNIa. Analysis of the observational data indicates that the explosion is induced by the thermonuclear burning of premixed carbon–oxygen fuel. Such phenomenon usually takes place in degenerate stars, white dwarfs.

The mode of the explosive nuclear burning in supernovae is still a controversial issue, in spite of many years of the research in the field. Four decades ago, Arnett [1]

was the first to consider supersonic combustion, i.e. detonation, in supernovae. Later, Ivanova et al. [2] obtained a sub-sonic flame (deflagration) propagating in spontaneous regime with pulsations and a subsequent transition to detonation, while Nomoto et al. [3] considered the deflagration propagating due to convective heat transfer. Both detonation and deflagration have their merits and problems in explaining the supernova phenomenon (see, e.g. [4]). It is not clear if detonation succeeds or fails to develop, but it is clear that in any case the combustion must be much faster than it is suggested by the analysis of the propagation of a laminar one-dimensional flame.

From microscopic point of view one-dimensional nuclear flame is a wave described essentially in the same way as it was done by Zeldovich and Frank-Kamenetsky [5] in spite of complications introduced by nuclear kinetics and very high conductivity of dense presupernova matter. It is found that the conductive flame propagates in presupernova with the speed which is too slow to explain the supernova outburst correctly since the flame Mach number is of the order of one percent or less [6].

The fuel consumption can naturally be accelerated by the development of the instabilities inherent to the flame front. As it is explained in the classical paper by Landau [7, 8], the hydrodynamic instability leads to wrinkling or roughening of the front surface, and hence to an increase of its area with respect to the smooth front and consequently to an acceleration of the flame propagation. In some cases, observed in laboratory experiments like [9], when the LD instability is really strong (large density jump across the flame front, and the flame is freely expanding) such instabilities can lead to a transition from the regime of slow flame propagation to the regime of detonation. Since the flame propagates in gravitational

*Electronic address: glazyrin@itep.ru

†Electronic address: sergei.blinnikov@itep.ru

‡Electronic address: dolgov@fe.infn.it

field, and the burned ashes have lower density than the unburned fuel, the Rayleigh–Taylor (RT) instability is often considered to be the dominant instability governing the corrugation of the front [10–14]. The RT instability creates turbulent cascade providing an acceleration of the flame front. However it leads to additional difficulties in modeling the SN event [15–19].

It is well known [7, 8, 20, 21] that large portions of a slow planar flame front are unstable with respect to the large scale bending. This universal instability is called the Landau–Darrieus (LD) instability. For the wavelengths much longer than the flame thickness it does not depend, on complex processes which take place in the burning zone. Development of the LD instability depends only on the sign of $\Delta\rho = \rho_u - \rho_b$, where ρ_u and ρ_b are the densities of the unburned and burned “gases” respectively. The LD instability of the planar flame fronts with respect to large scale bending takes place if and only if $\Delta\rho > 0$.

The LD instability plays an important role in many physical phenomena such as the usual chemical burning of gases, explosive boiling of liquids [22], electroweak phase transitions [23], dynamics of thermally bistable gas [24], and thermonuclear burning in supernovae [25, 26]. The detailed consideration the of non-linear stage of the LD instability and the calculation of the fractal dimension of the flame front for this case is given by Blinnikov and Sasorov [27], Joulin [28]. It is interesting, and somewhat puzzling, that a similar dependence of the flame fractal dimension on the density discontinuity was found in the 3D SPH simulations of the flame subject to the RT instability [29].

Both LD and RT instabilities develop on scales much larger than the flame thickness and they can be successfully studied in the approximation of the discontinuous front. This approximation is not valid for another instability, first discovered by Zeldovich [30] in his investigation of the powder combustion. This instability originated from a strong temperature dependence of the reactions rates. As a result of that local fluctuations of the heating rate caused by the temperature fluctuations cannot be controlled by thermal conduction. This phenomenon can lead to a pulsating regime of the front propagation and to a renormalization of the mean front velocity [31]. Such instability can develop even for one-dimensional perturbations when the plane front preserves its shape. We denote it as TP (thermal-pulsational) instability. After publication of paper by Barenblatt et al. [32] TP instability was studied quantitatively in many works (for the list of references see the book [33]).

A very nice review on the SNIa physics is given in [34] (see also [35, 36]). There exist several scenarios of SNIa explosions. The most popular are the following: the single–degenerate scenario, the double–degenerate scenario, and the sub-Chandrasekhar mass explosion. In this paper the single degenerate scenario is considered.

The paper is organized as follows. In Section II a model of a white dwarf explosion is presented and the physical

conditions are discussed. In Section III the stationary propagating flame is considered analytically and numerically. The dependence of the results on nuclear reaction network is discussed. In Section IV artificial systems with switched off hydrodynamics are considered. The effect of secondary reaction on pulsations is considered. In Section V the stability of the flame under conditions close to those in a white dwarf is considered. We show that pulsations could exist in this system when the Zeldovich number is artificially increased. After it we make conclusions about stability of real flames.

II. THE MODEL

According to the single degenerate scenario a binary stellar system, which is a progenitor of the supernova, consists of a white dwarf (WD) and a non degenerate star. During accretion of matter on the WD it approaches the Chandrasekhar mass limit and at some moment becomes unstable. In the language of equation of state it happens because the adiabatic exponent approaches the critical value $\gamma \approx 4/3$. In the course of this process the temperature in the centre of the WD rises and nuclear burning of matter is ignited. According to evolutionary models, the matter consists of degenerate ^{12}C and ^{16}O nuclei. The temperature of ignition depends on the matter density and can be found in [37]. For $\rho \sim 10^9 \text{ g/cm}^3$ it is about $T \sim 10^8 \text{ K}$. But this burning is very slow and does not propagate outwards from the centre until its energy release stops to be compensated for by various losses (the most significant are the neutrino losses). The dynamical stage sets in later, when T rises up to 10^9 K and the flame is born. This is the beginning of the supernova explosion. The flame starts to propagate from the centre of the star to its surface. The regime of the flame propagation is under intensive investigation but the answer is not yet found. Still it is not fully unknown, the observations imply some limitations on it. There exist two types of stationary regimes: 1) deflagration, when the flame propagation velocity is small compared to the speed of sound and the flame is driven by dissipative effects: thermo-conductivity or diffusion; 2)detonation, when a supersonic wave propagates with the shock front where the temperature jumps up drastically leading to fast burning. If the burning of the whole star proceeds in the detonation regime, it burns up to Fe-peak elements. However, it contradicts observations: in a real supernova about half of the star should consist of the intermediate elements. Pure deflagration regime does not succeed too: the star expands with velocity, which is faster than the flame velocity so the temperature drastically drops down and all the burning terminates. The only feasible successful regime is the mixed one when the flame starts with deflagration in high density matter, where the expansion coefficient is small. Then it somehow accelerates at the radius, which is usually characterized by some critical density, and passes to detonation. This model success-

fully explains all the parameters of the explosion at the expense of one tuning parameter, critical density, ρ_{crit} . From comparison of simulations with observations it is found that $\rho_{\text{crit}} \sim 2 \cdot 10^7 \text{ g/cm}^3$ (see, e.g. [34, 38]). But the global problem in SNIa physics (that is surely not solved in this paper) is to construct the model of the explosion with no tuning parameters. One should calculate the critical density of the burning regime transition from the first principles. This is the problem for the future.

Let us discuss physical conditions in a white dwarf assuming that its mass is close to the Chandrasekhar mass limit. The density in the centre of WD is $\rho \sim 10^9 \text{ g/cm}^3$. The chemical composition is mainly ^{12}C and ^{16}O . Hence it can be shown that the temperature at which the flame starts burning is about $T \sim 10^9 \text{ K}$. Two main physical processes that matter in the SNIa explosions are thermo-conductivity and nuclear reactions (burning). In this case ions are non-degenerate and non-relativistic, electrons on the contrary are strongly or semi-degenerate and relativistic. EOS for such matter is presented in [39] and takes into account ions and all degrees of degeneracy of electrons and photons.

Under these conditions the thermo-conductivity plays the leading role with respect to other dissipative processes. There are two components of the conductivity, radiative and electronic ones. The electronic thermo-conductivity was calculated in [40, 41]. An approximate equations for radiative thermo-conductivity are presented in [42]. We evaluate the magnitude of the diffusion effects in the star under scrutiny as follows, Despite the fact that in the white dwarf the matter is well mixed, we estimate the value of the ion diffusion coefficient as:

$$D \sim \lambda_i v_T, \quad (1)$$

where v_T is the thermal speed of the ions and λ_i is the ion mean free-path, which may be crudely estimated as the inter-ion distance. So the Lewis number, the relation between thermoconductivity (the coefficient is κ) and diffusion, is about $\text{Le} \equiv \kappa/\rho C_p D = 10^4$. Here C_p is heat capacity under constant pressure. This result can be easily explained by the differences of velocities of the relativistic particles, which contribute to thermoconductivity, and the non-relativistic ones, which contribute to diffusion. The shear viscosity can be written as:

$$\eta = mn\lambda_i v_T. \quad (2)$$

Where m and n are mass and concentration of ions. So the Prandl number, the relation between thermoconductivity and viscosity, is $\text{Pr} \equiv C_p \eta / \kappa = 10^{-4}$.

At the temperatures specified above, the nuclear reactions proceed in a branched network with a lot of isotopes. Let us assume for simplicity that WD consists only of ^{12}C . Then the first reaction in the nuclear network is $^{12}\text{C} + ^{12}\text{C} \rightarrow ^{24}\text{Mg}^*$, where Mg^* is an excited nuclei, which is unstable and decays into 3 channels with p , n , or α in the final states. Its caloricity is $q = 5.6 \cdot 10^{17} \text{ erg/g}$, so it leads to a significant temperature rise, up to $T \sim 10^{10}$

K, and can provoke further burning. In this paper two variants of nuclear network are considered:

1. A simplified network with only one reaction $^{12}\text{C} + ^{12}\text{C} \rightarrow ^{24}\text{Mg}^*$ (its rate can be found in [43]). According to the fact that it is the first reaction in the network and due to the electromagnetic nature of this reaction it could be a good approximation for the whole network, so all kinetics would be determined by this reaction. The complete burning up to Ni could also be modeled in this framework by fixing the rate and changing the caloricity to $q = 9.2 \cdot 10^{17} \text{ erg/g}$. The explicit expressions for species production rates and energy generation for this network are:

$$\begin{aligned} R_{\text{C12}} &= -F_{\text{scr}} A_{\text{C12}}^{-1} \rho X_{\text{C12}}^2 R(T), & (3) \\ R_{\text{Mg24}} &= -R_{\text{C12}}, \\ \dot{S} &= q R_{\text{Mg24}}, \\ R(T) &= 4.27 \cdot 10^{26} \frac{T_{9A}^{5/6}}{T_9^{1.5}} e^{-84.165/T_{9A}^{1/3} - 2.12 \cdot 10^{-3} T_9^3}, \\ T_{9A} &\equiv \frac{T_9}{1 + 0.0396 T_9}. \end{aligned}$$

For definitions see system (4). A_{C12} is the atomic mass of ^{12}C , F_{scr} is the screening factor (see below), T_9 is temperature in units of 10^9 K .

2. α -chain with 13 isotopes from [44]. We call it ‘‘APROX13’’. This nuclear network is supplied with the code that calculates R_i and \dot{S} .

We make an additional simulations with initial ^{16}O composition using APROX13. Because of the high matter density the degeneracy parameter is not small, $\Gamma \sim E_{\text{coul}}/E_{\text{kin}} \sim 1$ (where E_{coul} is a typical Coulomb energy per ion, and E_{kin} is a typical kinetic energy per ion), so the electron nuclear screening effects should be taken into account. The accurate screening factor F_{scr} in a non-ideal gas can be obtained only by Monte-Carlo simulations, and is presented, e.g., in [45]. We should emphasize that many-orders of magnitude discrepancy in the screening factor can arise because of incorrect definitions, see details in [41]. In our simulations the screening factor ranges from $F_{\text{scr}} \approx 10$ in unburned matter to $F_{\text{scr}} \approx 1$ in the ashes (F_{scr} exponentially depends on $1/T$).

Based on the consideration presented above we conclude that the stellar explosion can be described by the

following system of hydrodynamic equations:

$$\begin{aligned}
\frac{d\rho}{dt} &= -\rho \frac{\partial v}{\partial x}, \\
\frac{dX_i}{dt} &= R_i, \\
\frac{dv}{dt} &= -\frac{1}{\rho} \frac{\partial p}{\partial x}, \\
\frac{d\epsilon}{dt} &= -\frac{p}{\rho} \frac{\partial v}{\partial x} - \frac{1}{\rho} \frac{\partial Q}{\partial x} + \dot{S}, \\
Q &= -\kappa \partial_x T, \\
\dot{S} &= \sum R_i B_i, \\
p &= p(\rho, X_i, \epsilon),
\end{aligned} \tag{4}$$

which we need to solve. Here $X_i \equiv \rho_i/\rho$ are nuclide mass fractions ($i=\text{C12, Mg24}$ etc.), ϵ is internal energy per unit mass, R_i is the rate of production of species i , \dot{S} – energy generation rate, B_i – binding energies of species i .

Though we consider processes in a star, the system whose dynamics is crucially affected by gravity, the gravitational force is not included in the system (4). As it will be seen further, the thickness of the flame is negligible in comparison with scales of variation of gravitational force. So gravity does not have an impact on flame structure and all processes on the spatial scale of flame thickness.

III. PROPERTIES OF ONE-DIMENSIONAL FLAME

A. Formulation of the Problem

The main questions we pose here are the following: what is the normal velocity of flame propagation, what is the expansion coefficient of matter over the flame front, and what are the physical parameters of matter after the flame traversal. To answer these questions we should study microphysics of the plane burning front taking into account the processes with characteristic scale of the order of the front thickness.

Let us make some analytical estimations. For the deflagration regime the characteristic times of burning τ_{nucl} and heat transfer τ_{cond} over the front are respectively:

$$\tau_{\text{nucl}} = \frac{\rho q}{\dot{S}}, \quad \tau_{\text{cond}} = \frac{d^2}{\kappa}. \tag{5}$$

If the flame is stationary, these times should be equal, and we can estimate the flame thickness d and velocity as:

$$d = \sqrt{\kappa \frac{\rho q}{\dot{S}}}, \quad v = \frac{d}{\tau_{\text{cond}}} = \sqrt{\kappa \frac{\dot{S}}{\rho q}}. \tag{6}$$

In table I the estimated velocity values are presented for different conditions in WD, when the rate of burning \dot{S} is determined by the single reaction proposed earlier, ($2^{12}\text{C} \rightarrow 2^4\text{Mg}^*$).

Table I: Theoretical estimate of the front velocity and thickness with $2^{12}\text{C} \rightarrow 2^4\text{Mg}^*$ (Eqns. (5)–(6)):

ρ , g/cm ³	v , km/s	Δx , cm
$2 \cdot 10^8$	203	$2.5 \cdot 10^{-5}$
$7 \cdot 10^8$	742	$3.0 \cdot 10^{-6}$
$2 \cdot 10^9$	1300	$1.0 \cdot 10^{-6}$

The exact front parameters can be obtained only by the numerical simulations of system (4) in 1D. For general rates, R_{ij} , of the reactions in system (4) the density and temperature distributions in a steady burning wave are unknown, so the initial conditions with the steady flame could not be imposed. We simulate the ignition of the the flame by a warm wall and try to eliminate all interfering perturbations. We expect that the stationary flame would naturally appear in such conditions.

The numerical calculations are made for the following model conditions. The region of interest is supposed to consist of uniformly distributed matter. For simplicity it is assumed to be ^{12}C with density ρ_0 and temperature T_0 , chosen so that the characteristic time of the flame burning is much larger than the dynamical time in the problem under consideration. In this case the ignition is controlled by the boundaries. The right hand side boundary condition sets a constant external pressure. The left hand side boundary condition is a hard wall with the vanishing velocity, $v = 0$, and with the temperature linearly rising up to T_1 :

$$T(x=0) = \begin{cases} T_0 + \frac{T_1 - T_0}{\tau} t, & t < \tau \\ T_1, & t \geq \tau. \end{cases} \tag{7}$$

The choice of τ is specified below. T_1 is the temperature which is larger than the temperature of the active burning. All these quantities depend on the task and are tuned "by hand" after inspection of the trial values in each case. Let L be the size of the region of interest (it is smaller than the whole region of calculation). The burning leads to the temperature growth and therefore the pressure rises as well, which in turn generates sound waves. For the sake of avoiding unnecessary perturbations we should give time for sound waves to leave the region of interest, i.e. we demand that $\tau \gg L/c_s$. In this case the pressure in region L is constant with a good accuracy. The region $[0; L]$ is the region of interest, that is we observe flame propagation only there. This region contains uniform numerical grid and is only a part of the whole calculational domain $[0; L_0]$, filled with the nonuniform mesh, so that $L \ll L_0$, $L_0 > c_s t_{\text{simul}}$, where t_{simul} is the whole time of simulation. Under these conditions the right boundary does not play any role in the flame propagation.

Let us describe the numerical method for the solutions of system (4). Physically, the system consists of 3 parts: hydrodynamics, thermo-conductivity, and burning. For

solution we will use the method of splitting of physical processes. As an example let us consider the equation for energy ϵ in system (4). At each time step the equation is split as:

$$\frac{d\epsilon}{dt} = \left(\frac{d\epsilon}{dt}\right)_{\text{hydr}} + \left(\frac{\partial\epsilon}{\partial t}\right)_{\text{nucl}} + \left(\frac{\partial\epsilon}{\partial t}\right)_{\text{thermocond}}, \quad (8)$$

$$\left(\frac{d\epsilon}{dt}\right)_{\text{hydr}} = -\frac{p}{\rho} \frac{\partial v}{\partial x}, \quad (9)$$

$$\left(\frac{\partial\epsilon}{\partial t}\right)_{\text{nucl}} = \dot{S}, \quad (10)$$

$$\left(\frac{\partial\epsilon}{\partial t}\right)_{\text{cond}} = \frac{\partial(\kappa\partial_x T)}{\partial x}. \quad (11)$$

These equations are solved in 3 sub-steps: the hydrodynamic part in which $X_i = \text{const}$ and no energy generation is assumed; the nuclear part, ($\rho, v = \text{const}$), and the thermo-conductivity part, ($\rho, X_i, v = \text{const}$).

For the solution of hyperbolic PDE's we use the implicit lagrangian numerical scheme written in massive coordinates ($ds \equiv \rho dx$) and described in [46]. The quadratic artificial viscosity is implemented to make the possibility to calculate sharp discontinuities. Parabolic PDE (11) is solved with Crank–Nicholson numerical scheme. The kinetic equation for X_i with simplified nuclear network can be easily integrated analytically for a small time step. The APROX13 nuclear network has its own integrator.

Criteria that are used for determination of time and space discretization of parameters are the following:

$$\Delta t = \min_i(\Delta t_{\text{courant},i}, \Delta t_{\text{nucl},i}), \quad (12)$$

where $\Delta t_{\text{courant},i}$ is the Courant condition for i -cell and $\Delta t_{\text{nucl},i}$ is the time step at which all reagent concentrations change not more than by 1%.

B. Results of simulations

Here we present results of the computations. The approach we use here is very close to those used in the paper by [6]. The flame speed is determined by the time evolution of the position of the front centre, $x(t)$. By definition it is the point, where $X_{C12} = 0.5$. The medium is on the first stage heated with increasing temperature of the wall. At some moment the temperature rise becomes due to nuclear reactions and the flame born detaches from the left wall (its subsequent evolution does not depend on processes at the wall): the temperature of burned matter exceeds T_1 , and the characteristic timescale τ_{nucl} of the flame is smaller than τ . For additional study of independence of results on flame ignition see the Appendix A.

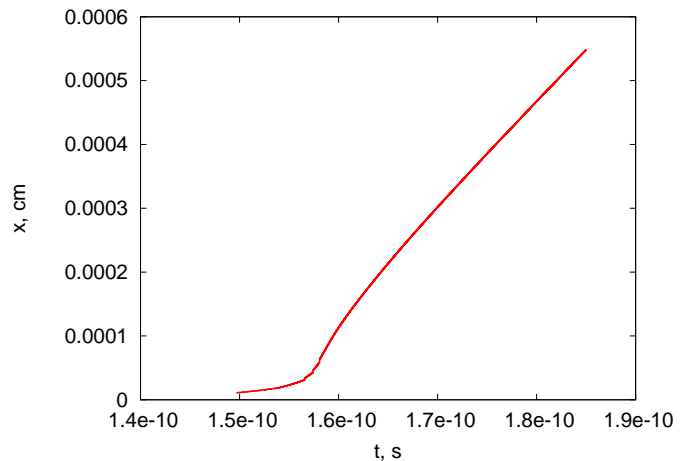


Figure 1: An example of the front coordinate dependence on time for $\rho = 2 \cdot 10^9 \text{ g/cm}^3$, initial composition ^{12}C , APROX13 nuclear network is used.

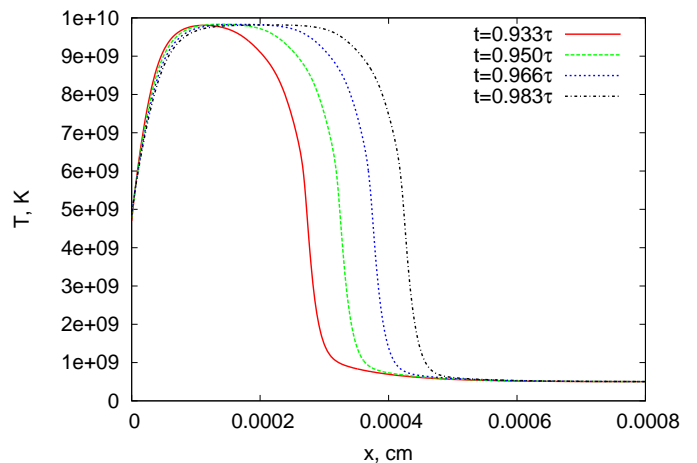


Figure 2: Sequential profiles of temperature for $t_1 < t_2 < t_3 < t_4$, $\rho = 2 \cdot 10^9 \text{ g/cm}^3$, initial composition ^{12}C , APROX13 nuclear network

An example of the time dependence, $x(t)$, is presented in Fig. 1. In Fig. 2 the coordinate dependence of the temperature for a sequence of times is shown. We see that some time after the ignition the flame stabilizes and propagates with constant velocity. Fitting the $x(t)$ dependence we obtain the velocity of flame relative to the wall, v . The normal flame velocity is then $v_n = \rho_b v / \rho_u$. Table II presents the results of the simulations for different initial states of matter for all nuclear network variants.

Fig. 3 shows the coordinate dependence of X_i for different elements at fixed time for APROX13 (flame moves from left to right). We see that the state close to nuclear quasi-equilibrium is set after some time of burning (see region $1 \cdot 10^{-4}$ to $2 \cdot 10^{-4}$ cm on Fig. 3, the chemical composition near point $x = 0$ is perturbed significantly by boundary condition). The numerically obtained re-

Table II: Results of the flame simulations. ρ_0 – initial density, “Calor.” – the variant of used nuclear network (for details see the text), T_{\max} – the temperature of burned matter, ρ_u/ρ_b – the ratio of unburned and burned matter densities, v_n – the normal flame velocity, Δx_{fr} – the flame width (determined by characteristic length of temperature rise), v_{TW} – flame velocity by Timmes & Woosley fit functions (should be compared with APROX13 velocities). The table also presents characteristic timescale of burning $\Delta x_{\text{fr}}/v_n$ for our results and those by TW (v_n obtained by Eqs. (43), (44) in TW, flame width by interpolation of Tables 3–4).

Compos.	ρ_0 , g/cm ³	Calor.	T_{\max} , 10 ⁹ K	ρ_u/ρ_b	v_n , km/s	Δx_{fr} , cm	$\Delta x_{\text{fr}}/v_n$, s	v_{TW} , km/s	$(\Delta x_{\text{fr}}/v_n)_{\text{TW}}$, s
¹² C	$2 \cdot 10^8$	Mg	6.9	1.54	70.1	$1.7 \cdot 10^{-4}$	$2.4 \cdot 10^{-11}$	26.7	$5.1 \cdot 10^{-10}$
		Ni	7.9	1.85	122	$1.2 \cdot 10^{-4}$	$9.8 \cdot 10^{-12}$		
		APROX13	6.8	1.60	18.2	$3.0 \cdot 10^{-4}$	$1.6 \cdot 10^{-10}$		
	$7 \cdot 10^8$	Mg	9.1	1.33	302	$1.8 \cdot 10^{-5}$	$6.0 \cdot 10^{-13}$	73.2	$2.9 \cdot 10^{-11}$
		Ni	10.7	1.57	470	$1.5 \cdot 10^{-5}$	$3.2 \cdot 10^{-13}$		
		APROX13	8.5	1.35	55.4	$4 \cdot 10^{-4}$	$7.2 \cdot 10^{-11}$		
	$2 \cdot 10^9$	Mg	11.3	1.26	854	$5.5 \cdot 10^{-6}$	$6.4 \cdot 10^{-14}$	170	$2.2 \cdot 10^{-12}$
		Ni	13.8	1.40	1241	$1.0 \cdot 10^{-5}$	$8.1 \cdot 10^{-14}$		
		APROX13	9.8	1.23	134	$1 \cdot 10^{-4}$	$7.5 \cdot 10^{-12}$		
¹⁶ O	$2 \cdot 10^8$	APROX13	6.1	1.38	0.94	$2 \cdot 10^{-2}$	$2.1 \cdot 10^{-7}$	2.0	$1.3 \cdot 10^{-7}$
	$2 \cdot 10^9$	APROX13	8.8	1.17	22.1	$5 \cdot 10^{-4}$	$2.3 \cdot 10^{-10}$	23.0	$1.5 \cdot 10^{-10}$

sults for 1-step nuclear network are in good agreement with analytical estimates (table I). The flame speed obtained with APROX13 show that the flame speed is about an order of magnitude slower, compared to one-step reaction. It is an important result showing that the pure carbon burning to Mg is not a good approximation, despite the fact that it dominates at early stages of the burning (see Fig. 3).

The flame speed obtained with APROX13 (which is supposed to be the real speed) can be calculated analytically if we substitute the rate of reaction $^{24}\text{Mg}(\alpha, \gamma)^{28}\text{Si}$ into Eq. (6) instead of $2\text{C} \rightarrow \text{Mg}$. The speed should decrease by the factor $\sqrt{R_{\text{CMg}}(T_9 \approx 10)/R_{\text{MgSi}}(T_9 \approx 10)} \sim 10$. This result is in accordance with the numerical simulations. Reactions with α particles dominate the whole burning and have more or less the same rates (the charge Z of heavy ions in the governing reactions does not vary significantly), so this estimate is accurate for all α -reactions.

Comparing our results with those of [6], here we mean only comparison with APROX13 nuclear network, we can see a good (but not excellent) agreement of 20%–30% (the worst case is the lowest density). Opacities and thermo-conductivities are the same in both papers. The difference could be caused by different nuclear rates: e.g., the $^{12}\text{C}(\alpha, \gamma)^{16}\text{O}$ reaction rate was changed since TW paper (F.X. Timmes, private communication). We have checked the impact of this change on our results and see no difference: 134 km/s vs 134 km/s for $\rho = 2 \cdot 10^9$ g/cm³, ^{12}C run. Nevertheless, due to uncertainties in Coulomb integral and nuclear network rates the speed of flame in SNIa is known with accuracy within a few tens of percent.

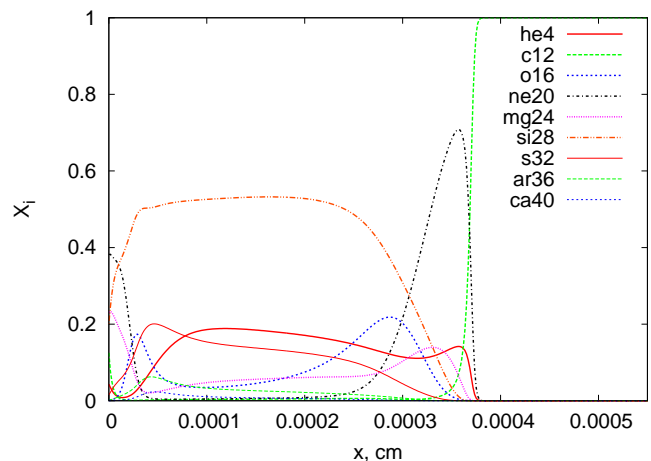


Figure 3: Coordinate dependence of concentrations of different elements for APROX13 nuclear network, $\rho = 2 \cdot 10^9$ g/cm³, initial composition ^{12}C

IV. THERMAL INSTABILITY OF NUCLEAR FLAMES

Let us consider now the thermal-pulsational instability with switched-off hydrodynamics. Due to absence of sonic waves in this case, this instability can be described without interference with other physical phenomena. Two conditions are necessary for the development of the TP instability [31, 33]. First, the thermal diffusion must be more than an order of magnitude larger than the mass diffusion. This condition is undoubtedly satisfied in presupernovae where $\text{Le} \gg 1$. Second, the Zeldovich number [47]:

$$\text{Ze} = \left(\frac{\partial \ln \dot{S}}{\partial \ln T} \right)_{P, X_i}, \quad (13)$$

which characterizes the temperature dependence of the heating rate \dot{S} , must be high enough. Here P is the pressure, X_i ($i = 1, 2, \dots$) are the abundances of the reactants, and the derivative is evaluated at the temperature of the burned matter (ashes). The thermal instability takes place when Ze is higher than a certain critical value Ze_{cr} . From the Arrhenius law, and in the approximation when the reaction zone is assumed to be negligibly thin in comparison to the preheat zone of the flame, it is found that $Ze_{cr} = 4 + 2\sqrt{5} = 8.47$ [33]. The recent numerical value [48], obtained by relaxing the approximation of delta function kinetics, is $Ze_{cr} \simeq 8.24 - 8.29$.

When Ze is below the critical value, the front velocity relaxes quickly to a constant value, but when it is larger than Ze_{cr} the pulsations set in. This is illustrated in Fig.4.

This plot shows the result of the integration of the following simplified system (compared to Eqns. (4) κ and B_i are taken to be unity):

$$\frac{\partial T}{\partial t} = \frac{\partial}{\partial x} \left(\frac{\partial T}{\partial x} \right) + RX_A^2. \quad (14)$$

Here, we assume that the kinetic equation is

$$\frac{dX_A}{dt} = -RX_A^2, \quad (15)$$

and the rate of the reaction $R = R(T)$ is taken as

$$R = \exp \left(-E_a \left(\frac{1}{T} - \frac{1}{T_0 + 1} \right) \right). \quad (16)$$

In our units the initial temperature is T_0 , ashes have temperature $T_b = T_0 + 1$ and the activation energy is

$$E_a = Ze \frac{T_b}{T_b - T_0} = Ze(1 + T_0). \quad (17)$$

We have used the method of lines to simulate the solution of the equation of thermal conduction. Namely, the space coordinate was discretized by finite differences, while integration over time was done by ODE integrators using methods of [49] and [50]. See details of the numerical technique in more complicated situation of hydrodynamical evolution in [51]. Our simulations for this simple model give $Ze_{cr} \simeq 8.2$.

In order to get insight in more complicated simulations of nuclear flames discussed in Section VI we have introduced another reactant in our set of equations.

Instead of a large kinetic scheme of many reactions we use a simplified two-reactant system, which allows us to do simple numerical experiments, elucidating the role of secondary reactions (“A” is like carbon, and “B” like He - initially He is 0 and appears as a result of C-burning; the reaction A+B has lower Coulomb barrier, than A+A, hence lower E_a ; the system is not closed, reactions burn to some ashes not included in the system; all parameters and the system are artificial):

$$\frac{\partial T}{\partial t} = \frac{\partial}{\partial x} \left(\frac{\partial T}{\partial x} \right) + \left(\frac{3}{2} - \frac{1}{2}q_2 \right) R_1 X_A^2 + q_2 R_2 X_A X_B. \quad (18)$$

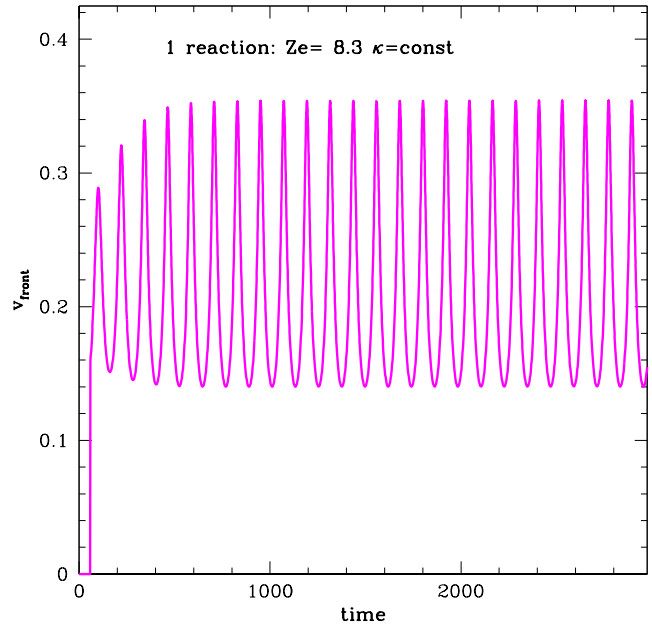


Figure 4: Pulsating front velocity for $Ze = 8.3$ and one reaction obeying the Arrhenius law with switched-off hydrodynamics

and assume the following kinetic equations:

$$\frac{dX_A}{dt} = -R_1 X_A^2 - R_2 X_A X_B, \quad (19)$$

$$\frac{dX_B}{dt} = +\frac{1}{2} R_1 X_A^2 - R_2 X_A X_B, \quad (20)$$

where the reaction rates, $R_i = R_i(T)$, are taken as

$$R_1 = \exp \left(-E_a \left(\frac{1}{T} - \frac{1}{T_0 + 1} \right) \right), \quad (21)$$

and

$$R_2 = \exp \left(-\frac{E_{a2}}{T} + \frac{E_a}{T_0 + 1} \right). \quad (22)$$

Thus the first reaction has activation energy E_a while the second one has activation energy E_{a2} . Changing E_{a2} we are able to study the effect of secondary reaction on the stability of the flame, when Ze -number is determined by the primary reaction.

Models presented in this section are artificial, but they can show the variety of effects in systems with burning.

Figs. 5-7 illustrate, that for $Ze=12$ the secondary reaction stabilizes the flame, but for large enough Ze -number the instability can develop even when the presence of the secondary reactions.

Examples in this section were given for the case of the switched-off hydrodynamics. Now we turn to the flames with an account of hydrodynamics, which is a better approximation for realistic supernovae.

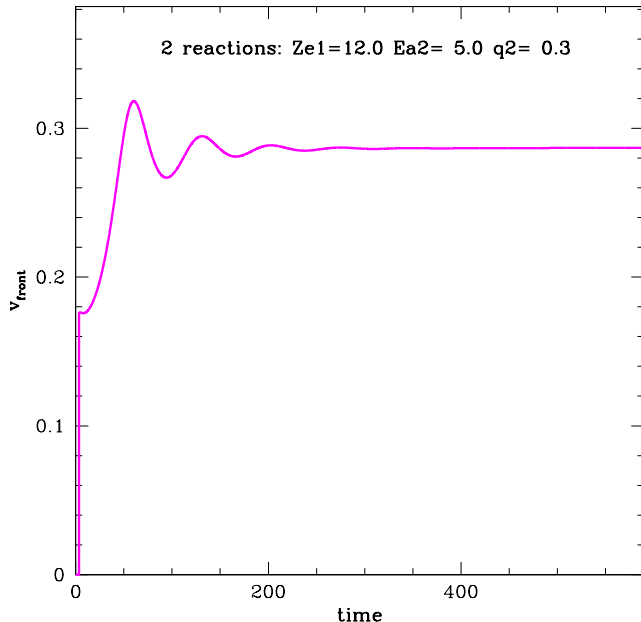


Figure 5: Pulsating front velocity for $Ze = 12$ and a two-reaction artificial network with switched-off hydrodynamics

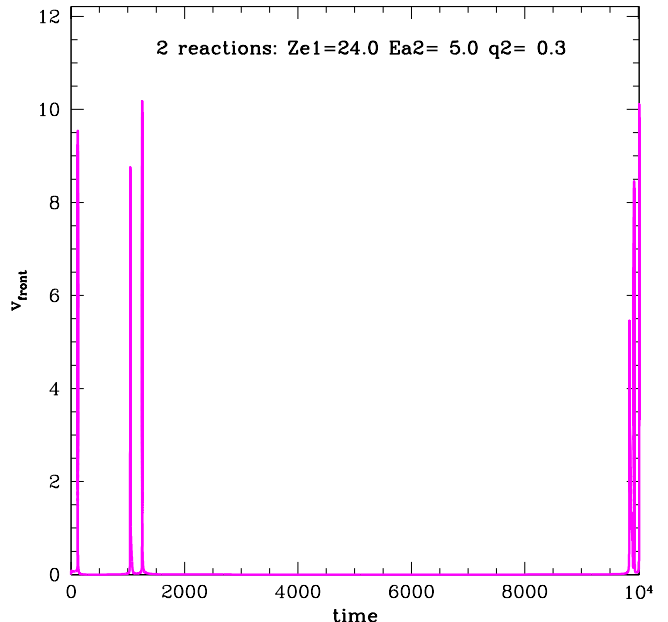


Figure 7: Pulsating front velocity for $Ze = 24$ and a two-reaction artificial network with switched-off hydrodynamics

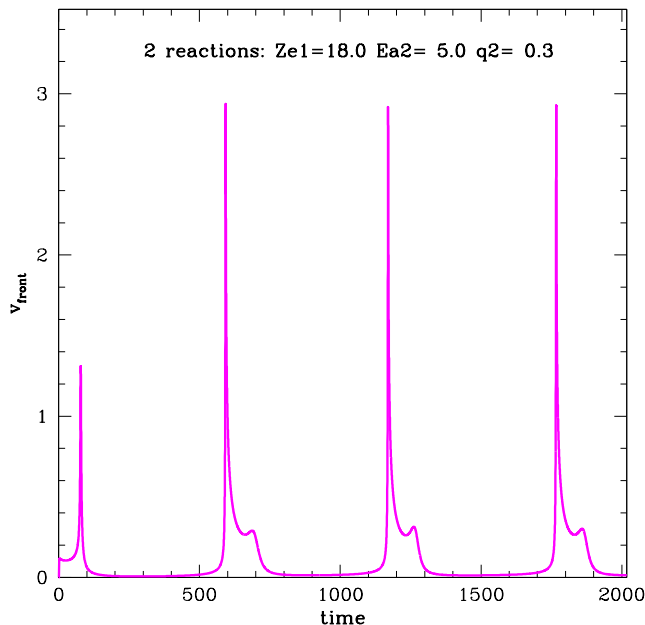


Figure 6: Pulsating front velocity for $Ze = 18$ and a two-reaction artificial network with switched-off hydrodynamics

V. FRONT PULSATIONS

Here we will switch on hydrodynamics again. According to the simulations in Section III with the full set of reactions the instability was not observed (see the text below). Now we show that pulsational behaviour can exist in our simulations in the case of artificially high Zeldovich numbers and by that will confirm that carbon and oxygen burning are stable. Here we should mention that the only source of fluctuations in our system is numerical noise and we can detect the pulsational regime only if its frequency is resolved by our numerical scheme. Looking back to our paper [52], where the results of numerical simulations of some toy model coincide with analytical consideration very well, we hope to detect real pulsations in this system too. To carry out this task we should change the nuclear rate function. We treat the reactions as one-step process with the rate given by the Arrhenius law:

$$R(T) = Ae^{-\mathcal{B}/T_9}. \quad (23)$$

Constant \mathcal{B} determines the Zeldovich number, Ze , according to eq. (13):

$$Ze_{\text{Arren}} = \frac{\mathcal{B}}{T_{9 \text{ burned}}}, \quad (24)$$

where $T_{9 \text{ burned}}$ is the temperature of the burned matter (ashes).

One of the goal of this Section is to show the possibility to resolve pulsations in numerical codes like ours.

The proposed simplified one-step reaction with Arrhenius rate is the way to parameterize the Zeldovich number. Changing \mathcal{B} we simply change \mathcal{Z} .

The value of constant A does not play any role here, but for definiteness we determine it by the relation:

$$\int_{T_1}^{T_2} R(T_9) dT_9 = \int_{T_1}^{T_2} R_{\text{real}}(T_9) dT_9, \quad (25)$$

$$A(\mathcal{B}) = \int_{T_1}^{T_2} R_{\text{real}}(T_9) dT_9 \left(\int_{T_1}^{T_2} e^{-\mathcal{B}/T_9} dT_9 \right)^{-1}. \quad (26)$$

For $R_{\text{real}}(T)$ we take the rate of the considered above simplified nuclear network.

The nuclear caloricity is taken from nuclear transformations $^{12}\text{C} \rightarrow ^{24}\text{Mg}$ and $^{12}\text{C} \rightarrow ^{56}\text{Ni}$ (the used value will be denoted in each simulation explicitly in the data table). According to the results of the previous section we set the boundary temperatures as $T_1 = 1$, $T_2 = 10$. Fig. 8 shows different rates used, compared to the “real rate”. We see that the rate with $\mathcal{B} \approx 50$ fits the physical carbon burning rate very nicely. This means that when $T_{9\text{up}} \approx 10$, $\mathcal{Z} \approx 5$, which coincides with estimates presented in Section VI. Table III presents the results for different runs with $\rho_0 = 2 \cdot 10^9 \text{ g/cm}^3$. We increase \mathcal{B} from 20 to 200 and simultaneously decrease caloricity q (from Ni to Mg) to avoid the flame acceleration. We see that for the normal caloricity ($q = (5.6 - 9.2) \cdot 10^{17} \text{ erg/g}$) no pulsations appear for all variants of rates (upper part of the table). Zeldovich number, \mathcal{Z} , can be additionally increased by decreasing $T_{9\text{burned}}$. This is done by the caloricity change to $q = 5 - 7 \text{ MeV}$ for one reaction ($q = (2.0 - 2.8) \cdot 10^{17} \text{ erg/g}$). In this case pulsations appear for $\mathcal{B} > \mathcal{B}_{\text{crit}} \simeq 112.5$ (the lower part of the table). Example of the flame coordinate dependence is depicted in Fig. 9, and the corresponding evolution of temperature in Fig. 10. Additional variants were calculated for the intermediate caloricity $q = 3.5 \cdot 10^{17} \text{ erg/g}$. The results for this caloricity show the same Zeldovich number (within the uncertainties of results).

So the result is that in “real” system (physical EOS and thermoconductivity) pulsations can exist, but only in the case of unphysical values of the parameters. In particular, the Zeldovich number should be increased by a factor of ~ 4 . Table IV presents the critical values of \mathcal{Z} number found in our numerical experiments for different densities of matter.

In the case of complex nuclear network (many reactions) \mathcal{Z} number cannot be obtained in such straightforward way, because it depends on the whole history of burning $\dot{S}(T)$. The front is stable in simulations with APROX13, presented in Section III for all runs. The only run which indicates the instability, but in reality is stable, is with initial ^{16}O and $\rho = 2 \cdot 10^8 \text{ g/cm}^3$ (one from the bottom in Table II). It demonstrates some irregular structure in $x(t)$ dependence (see Fig. 11 and

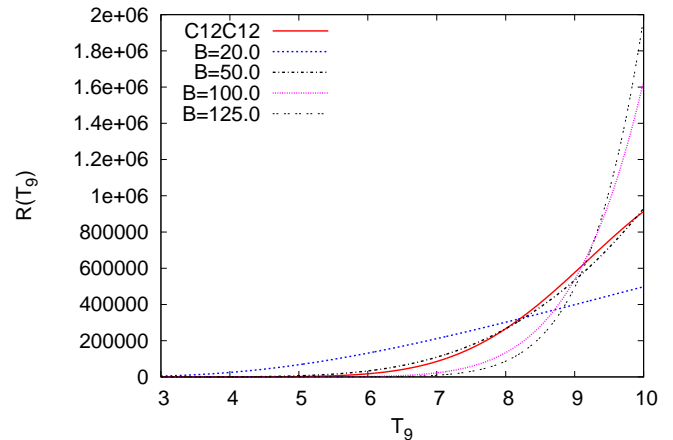


Figure 8: Comparison of artificial rates with $^{212}\text{C} \rightarrow \text{Mg}^{24}$ (in the plot keys \mathcal{B} is \mathcal{B})

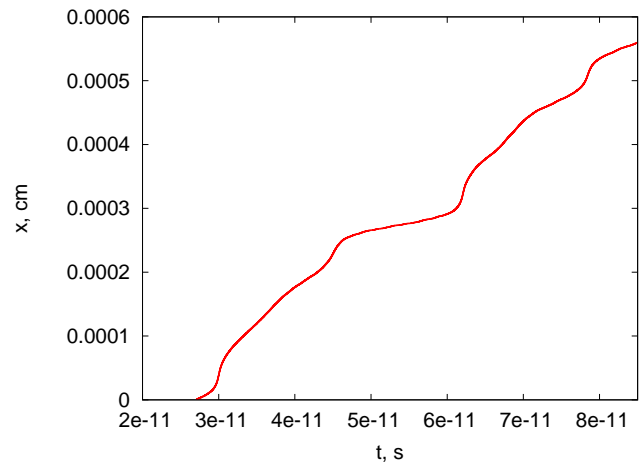


Figure 9: Pulsational regime of flame with artificially increased Zeldovich number, $\rho = 2 \cdot 10^9 \text{ g/cm}^3$, $\mathcal{B} = 112.5$, $q = 2.4 \cdot 10^{17} \text{ erg/g}$

compare to Fig. 9). This case is the best candidate for pulsations because of low T_b and strong temperature dependence. But the period of these pulsations, $\tau_1 \sim 3 \cdot 10^{-10} \text{ s}$, is not far from the numerical cell crossing time $\tau_2 = \Delta x \rho_b / (u_n \rho_u) = 1.5 \cdot 10^{-9} \text{ s}$ (here Δx is the size of a cell), and to check, whether it is a numerical effect, we perform simulation with different Δx , see Fig. 11. It could be seen that the period of pulsations decreases with the cell size together with the mean squared deviation from the linear law. So these pulsations are numerical and they do not contribute to physical effects like changing the flame velocity. Another signature of physical pulsations (not observed in this run), is that they appear not only in $x(t)$ dependence and also in pul-

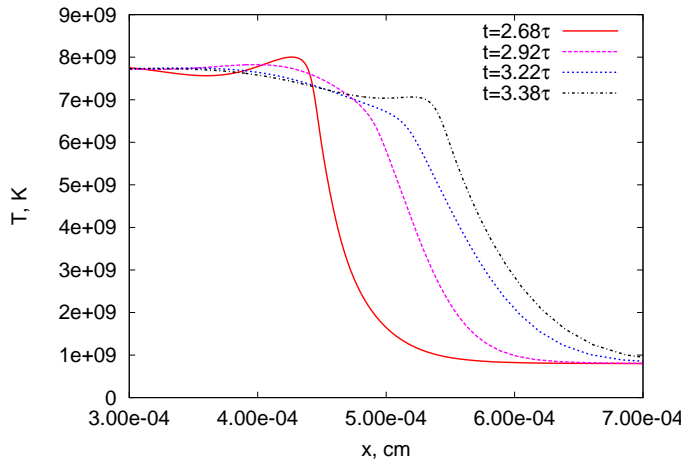


Figure 10: Temperature profiles for pulsational regime of flame with artificially increased Zeldovich number, $\rho = 2 \cdot 10^9$ g/cm³, $\mathcal{B} = 112.5$, $q = 2.4 \cdot 10^{17}$ erg/g

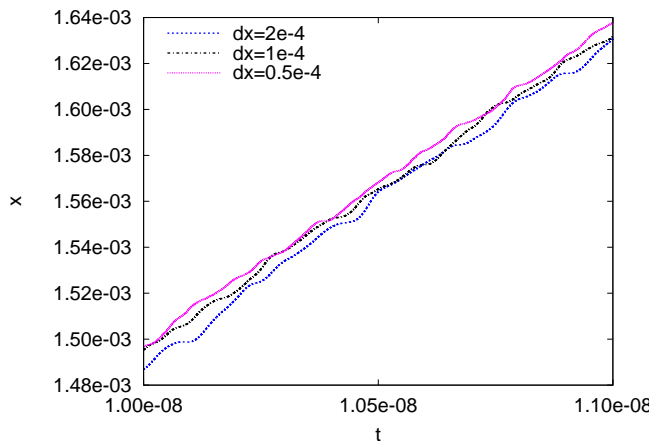


Figure 11: Flame coordinate for run with ¹⁶O, $\rho = 2 \cdot 10^8$ g/cm³, APROX13 network. Three runs with the same conditions but different resolution (cells size).

sations of T_{burned} in the same way as was shown in the paper by [52].

VI. DISCUSSION

Timmes and Woosley [6] simulated the flame fronts of different CO mixtures using one-dimensional time-dependent hydro code. They said nothing about the thermal-pulsational (TP) instability. At first glance this means that there is no TP instability in the degenerate presupernova conditions. However, later, Bychkov and Liberman [53] and Nomoto et al. [54] have argued that C+C and O+O flame fronts should be TP-unstable. In the approximation of delta function kinetics it is found

Table III: Results of simulations with Arrhenius law:

	A	\mathcal{B}	$q, 10^{17}$ erg/g	$T_{9\text{burned}}$	comm.
1	$3.68 \cdot 10^6$	20.0	9.2	13.5	flame
2	$1.38 \cdot 10^8$	50.0	9.2	13.5	flame
3	$7.62 \cdot 10^{12}$	150.0	5.6	11	flame
4	$1.47 \cdot 10^{15}$	200.0	5.6	14	deton.
5	$7.62 \cdot 10^{12}$	150.0	2.8	10	puls.
6	$3.60 \cdot 10^{10}$	100.0	2.8	8	flame
7	$5.32 \cdot 10^{11}$	125.0	2.8	8	puls.
8	$1.39 \cdot 10^{11}$	112.5	2.8	8.2	flame
9	$1.39 \cdot 10^{11}$	112.5	2.0	7.8	puls.
10	$1.39 \cdot 10^{11}$	112.5	2.4	8	puls.
11	$4.44 \cdot 10^{11}$	123.3	3.5	9.0	puls.
12	$3.11 \cdot 10^{11}$	120.0	3.5	9.0	flame

Table IV: Critical Zeldovich number for carbon burning at different densities (parameterized with the one-step reaction rate):

$\rho, \text{g/cm}^3$	$Z_{\text{e,cr}}$
$2 \cdot 10^8$	$18.4 < Z_{\text{e}} < 20.4$
$7 \cdot 10^8$	$14.6 < Z_{\text{e}} < 15.6$
$2 \cdot 10^9$	$13.5 < Z_{\text{e}} < 13.9$

in [53] that $Z_{\text{e,cr}} = 8 + 4\sqrt{5} = 16.9$. It is larger than Z_{e} calculated by the Arrhenius law exactly by factor 2 (and close to ours in Table IV). [53] even claimed that Timmes and Woosley [6] have overlooked the instability in their simulations.

We believe that the latter extreme proposition is not true and based on the results of the simulations presented above we put forward a different explanation of the apparent CO front stability. It is known that CO nuclear burning consists of the basic (C, α), (C,p), (O, α), ... reactions accompanied by secondary (p, γ) and (α , γ) reactions. It is very important that:

1. Z_{e} corresponding to the secondary reactions is rather low because of the lower height of the Coulomb barrier;
2. The amount of energy yielded by the secondary reactions is comparable to the yield of the basic ones.

It is very difficult to study analytically any model with many reactants. It should be made numerically as it was done in Section III and by Timmes and Woosley [6]. However, it is possible to develop a simple analytical model like in [52], [55] with *one* deficient reactant which possesses in part the main properties of CO burning mentioned above, and which can help to understand the qualitative behaviour of the pulsating front. Moreover, as we have shown in Section IV, it is not hard to develop a numerical model with only *two* reactions with different values of activation energies giving two Z_{e} numbers, one of them above and the other below the critical value.

This model explains how the seeming contradiction between works [53, 54], and the simulations in Ref. [6] can be removed.

The results of Section V show that for physical parameters of a white dwarf matter it is possible to obtain a pulsational regime of the flame propagation, but only in case of increased Zeldovich number. The Zeldovich number of a one-step reaction with Arrhenius law reflects the dynamics with similar net Zeldovich number (obtained by real $\dot{S}(T)$ history over flame) of a more complex network like aprox13. We determined the Ze number in results obtained by [6] (see their Fig. 3), evaluating the ratio of the thickness of the conductive zone to the thickness of the reaction zone which reflects the effective value of the Ze number [47]. We find this value in the range 2 – 5. This range is noticeably lowerer the critical value Ze_{cr} . This fact suggests the explanation for the stability of CO flame front observed by Timmes and Woosley [6]. Moreover, it shows that the secondary reactions of CO burning are very important from the viewpoint of the TP stability and that the models considered in [53, 54] are oversimplified.

[6] suggested electron captures as a stabilizing effect for the Rayleigh–Taylor instability. This effect do not have impact on pulsational instability because electron capture is a process with the time scale of weak processes $> 10^{-4}$ s. And the timescale of the pulsational instability is much smaller (see Table II).

VII. CONCLUSIONS

One-dimensional flame propagation in presupernova white dwarf has been considered. Flame properties for different star densities were obtained. It is shown that

when only one nuclear reaction in the nuclear network is considered, the flame velocity strongly differs from more sophisticated net simulations. So this simplified approach can be used only in approximate simulations when the exact value of the flame velocity is not required, or alternatively the nuclear rate should be adjusted to fit the correct value of v_n .

We have also studied one-dimensional pulsational instability. First, with artificial systems the switched-off hydrodynamics were considered. The possibility of secondary reactions to stabilize the front was shown with the help of this system (by decreasing the net Ze number).

In “real” simulations, presented in Section III no pulsation regime was found, so we used the simplified Arrhenius law in one-step reaction to make it possible to change Zeldovich number, Ze. For high Ze numbers the pulsations do exist. It means that our numerical code can resolve such pulsations and that they can exist in conditions close to “real”, but with steeper energy generation rate. By means of numerical simulations we have obtained critical Zeldovich numbers for densities in the range $\rho = [2 \cdot 10^8, 2 \cdot 10^9]$ g/cm³. These values are larger than those in real flame, which proves one-dimensional stability of the realistic flame fronts in supernovae.

Acknowledgements

We are grateful to V.Chechetkin, W.Hillebrandt, A.Kruzhilin, J.Niemeyer, P.Sasorov, S.Woosley, and F.Timmes for cooperation, discussions and references. MPA supported the work of SB in Germany. The work in Russia is supported by RFBR grants 11-02-00441-a and 13-02-92119, Sci. Schools 5440.2012.2, 3205.2012.2 and 3172.2012.2, by the contract No. 11.G34.31.0047 of the Ministry of Education and Science of the Russian Federation, and SCOPES project No. IZ73Z0-128180/1.

-
- [1] W. D. Arnett, *Astrophysics and Space Science* **5**, 180 (1969).
 - [2] L. N. Ivanova, V. S. Imshennik, and V. M. Chechetkin, *Astrophysics and Space Science* **31**, 497 (1974).
 - [3] K. Nomoto, D. Sugimoto, and S. Neo, *Astrophysics and Space Science* **39**, L37 (1976).
 - [4] S. E. Woosley and T. A. Weaver, *Annual Review on Astronomy and Astrophysics* **24**, 205 (1986).
 - [5] Y. B. Zeldovich and D. A. Frank-Kamenetsky, *Acta Physicochim. USSR* **9**, 341 (1938).
 - [6] F. X. Timmes and S. E. Woosley, *The Astrophysical Journal* **396**, 649 (1992).
 - [7] L. D. Landau, *ZhETF* **14**, 240 (1944).
 - [8] L. D. Landau, *Acta Physicochim. USSR* **19**, 77 (1944).
 - [9] Y. A. Gostintsev, A. G. Istratov, and Y. V. Shulenin, *Combust. Expl. Shock Waves* **24**, 563 (1988).
 - [10] E. Mueller and W. D. Arnett, *The Astrophysical Journal* **307**, 619 (1986).
 - [11] S. E. Woosley, in *Supernovae*, edited by A. G. Petschek (Springer, Berlin, 1990), pp. 182–212.
 - [12] S. E. Woosley, in *Gamma-Ray Line Astrophysics*, edited by P. Durouchoux and N. Prantzos (New York, 1991), vol. 232 of *AIP Conf. Proc.*, pp. 270–290.
 - [13] E. Livne and D. Arnett, *The Astrophysical Journal Letters* **415**, L107 (1993).
 - [14] A. M. Khokhlov, *The Astrophysical Journal* **419**, 200 (1993).
 - [15] J. C. Niemeyer and W. Hillebrandt, *The Astrophysical Journal* **452**, 769 (1995).
 - [16] J. C. Niemeyer, Ph.D. thesis, Technical University of Munich, also available as MPA-911 (1995).
 - [17] J. C. Niemeyer and S. E. Woosley, *ApJ* **475**, 740 (1997), arXiv:astro-ph/9607032.
 - [18] S. E. Woosley, A. R. Kerstein, V. Sankaran, A. J. Aspden, and F. K. Röpkke, *The Astrophysical Journal* **704**, 255 (2009), 0811.3610.
 - [19] A. J. Aspden, J. B. Bell, M. S. Day, S. E. Woosley, and M. Zingale, *The Astrophysical Journal* **689**, 1173 (2008), 0811.2816.
 - [20] L. D. Landau and E. M. Lifshitz, *Fluid Mechanics* (Pergamon Press: Oxford, 1959).
 - [21] A. Liñán and F. A. Williams, *Fundamental Aspects of*

- Combustion* (Oxford University Press, New York, 1993).
- [22] D. L. Frost, *Physics of Fluids* **31**, 2554 (1988).
- [23] M. Kamionkowski and K. Freese, *Physical Review Letters* **69**, 2743 (1992).
- [24] I. Aranson, B. Meerson, and P. V. Sasorov, *Physical Review E* **52**, 948 (1995).
- [25] S. I. Blinnikov, P. V. Sasorov, and S. E. Woosley, *Space Science Reviews* **74**, 299 (1995).
- [26] J. C. Niemeyer and W. Hillebrandt, *The Astrophysical Journal* **452**, 779 (1995).
- [27] S. I. Blinnikov and P. V. Sasorov, *Physical Review E* **53**, 4827 (1996).
- [28] G. Joulin, *Physical Review E* **50**, 2030 (1994).
- [29] E. Bravo and D. Garcia-Senz, *The Astrophysical Journal Letters* **450**, L17+ (1995).
- [30] Y. B. Zeldovich, *ZhETF* **12**, 498 (1942).
- [31] F. A. Williams, *Combustion Theory* (Benjamin/Cummings, Menlo Park, CA, Reading, MA, 1985).
- [32] G. I. Barenblatt, Y. B. Zeldovich, and A. G. Istratov, *Prikl.Mekh.Tekh.Fiz.* **4**, 21 (1962).
- [33] Y. B. Zeldovich, G. I. Barenblatt, V. B. Librovich, and G. M. Makhviladze, *The Mathematical Theory of Combustion and Explosions* (Consultants Bureau, New York, 1985).
- [34] W. Hillebrandt and J. C. Niemeyer, *Annual Review of Astronomy and Astrophysics* **38**, 191 (2000), arXiv:astro-ph/0006305.
- [35] F. K. Röpke, W. Hillebrandt, and S. I. Blinnikov, in *EPS-13 Conference "Beyond Einstein – Physics for the 21st Century"* (University of Bern, Switzerland, 2006), vol. 637 of *ESA Special Publication*, arXiv:astro-ph/0609631.
- [36] F. K. Röpke, W. Hillebrandt, W. Schmidt, J. C. Niemeyer, S. I. Blinnikov, and P. A. Mazzali, *The Astrophysical Journal* **668**, 1132 (2007), 0707.1024.
- [37] A. Y. Potekhin and G. Chabrier, *Astron. Astrophys.* **538**, A115 (2012), 1201.2133.
- [38] A. M. Khokhlov, E. S. Oran, and J. C. Wheeler, *The Astrophysical Journal* **478**, 678 (1997), arXiv:astro-ph/9612226.
- [39] S. I. Blinnikov, N. V. Dunina-Barkovskaya, and D. K. Nadyozhin, *The Astrophysical Journal Supplement Series* **106**, 171 (1996).
- [40] D. G. Yakovlev and V. A. Urpin, *Soviet Astronomy* **24**, 303 (1980).
- [41] S. I. Glazyrin and S. I. Blinnikov, *Journal of Physics A Mathematical General* **43**, 075501 (2010), 0907.0439.
- [42] I. Iben, Jr., *The Astrophysical Journal* **196**, 525 (1975).
- [43] G. R. Caughlan and W. A. Fowler, *Atomic Data and Nuclear Data Tables* **40**, 283 (1988).
- [44] F. X. Timmes, R. D. Hoffman, and S. E. Woosley, *The Astrophysical Journal Supplement* **129**, 377 (2000).
- [45] G. Chabrier and A. Y. Potekhin, *Physical Review E* **58**, 4941 (1998).
- [46] A. A. Samarskii and Y. P. Popov, *Finite-difference methods for solving hydrodynamical problems* (Nauka, Moscow, 1992).
- [47] P. Clavin, *Ann. Rev. Fluid Mech.* **26**, 321 (1994).
- [48] A. Bayliss and B. J. Matkowsky, *SIAM Journal on Applied Mathematics* **50**, 437 (1990).
- [49] C. W. Gear, *Numerical initial value problems in ordinary differential equations* (Engelwood Cliffs: Prentice-Hall, 1971).
- [50] R. K. Brayton, F. G. Gustavson, and G. D. Hachtel,

Table V: Parameters of simulations:

ρ , g/cm ³	T_0 , K	T_1 , K	L , cm	τ , s
$2 \cdot 10^8$			$9 \cdot 10^{-3}$	
$7 \cdot 10^8$	$5 \cdot 10^8$	$5 \cdot 10^9$	$2.4 \cdot 10^{-3}$	$1.8 \cdot 10^{-10}$
$2 \cdot 10^9$			$4.5 \cdot 10^{-4}$	

Table VI: Results of additional runs for testing impact of run parameters. The second column shows the parameter that was changed together with its new value. $(v_n)_{\text{new}}$ and $(v_n)_{\text{old}}$ are new and old values of normal flame velocity, respectively, ¹²C initial composition, aprox13 network.

ρ , g/cm ³	param. change	$(v_n)_{\text{new}}$, km/s	$(v_n)_{\text{old}}$, km/s
$2 \cdot 10^8$	$T_0 \rightarrow 7 \cdot 10^8$ K	18.6	18.2
	$T_1 \rightarrow 4 \cdot 10^9$ K	18.2	18.2
$2 \cdot 10^9$	$T_0 \rightarrow 7 \cdot 10^9$ K	136	134
	$T_1 \rightarrow 4 \cdot 10^9$ K	134	134

Proceedings of the IEEE **60**, 98 (1972).

- [51] S. I. Blinnikov and N. V. Dunina-Barkovskaya, *MNRAS* **266**, 289 (1994).
- [52] S. I. Glazyrin and P. V. Sasorov, *Monthly Notices of the Royal Astronomical Society* **416**, 2090 (2011), 1012.5982.
- [53] V. V. Bychkov and M. A. Liberman, *The Astrophysical Journal* **451**, 711 (1995).
- [54] K. Nomoto, K. Iwamoto, T. Shigeyama, and H. Takabe, in *"Laser interaction and related phenomena"* (New York, 1996), vol. 489 of *AIP Conference proceedings*.
- [55] R. O. Weber, G. N. Mercer, H. S. Sidhu, and B. F. Gray, *Proc. R. Soc. Lond. A* **453**, 1105 (1997).

Appendix A: Parameters of simulations

The parameters of all simulations are presented in Table V. The characteristic time of wall heating τ (see Eq. 7) has no impact on the results because the flame is born at times $t > \tau$ (except the variant when $\rho = 2 \cdot 10^9$ g/cm³, where $t \sim \tau$, but for this variant the flame transition time satisfies $L/v_n \ll \tau$, so it crosses the region of interest L with constant T_{left}). We have made several additional runs to check the dependence of our results on the initial and boundary temperatures. The results are presented in Table VI and show weak dependence of velocity on the initial temperature. It happens because higher T_0 leads to faster heating of unburned matter by thermo-conductivity to the temperature of active burning and by this leads to small increase of flame velocity.